Effects of bistramide A
on a non-small-cell bronchial carcinoma line

C. Roussakis[1], N. Robillard[2], D. Riou[1], J. F. Biard[1], G. Pradal[3], P. Piloquet[3], C. Debitus[4], and J. F. Verbist[1]

[1] Groupe de recherche "Substances marines à Activité Biologique" (SMAB), Faculté de Pharmacie, 1 rue G. Veil, F-44035 Nantes Cedex 01, France
[2] Service commun de cytométric en flux, Laboratoire d'Hématologie, CHR, F-44035 Nantes Cedex 01, France
[3] Laboratoire d'Histologie et Embryologie, UFR de Médicine, 1 rue G. Veil, F-44035 Nantes Cedex
[4] Laboratoire de Pharmacologie, ORSTOM, BP A5, Nouméa, Nouvelle-Calédonie

Summary. The antiproliferative effects of bistramide A, a nitrogenous dilactam polyether from *Lissoclinum bistratum* Sluiter (Urochordata), were studied at the level of the cell cycle in asynchronous cells of the NSCLCN6-L16 line. Bistramide A has a dual mechanism that induces blockade in the G1 phase (compatible with differentiation properties reported elsewhere) and causes polyploidy that is suggestive of inaptitude for cytokinesis. These effects confirm the results of cytomorphology studies in electron microscopy.

Introduction

The prospective development of a new antitumor drug requires that its mechanism of action be understood early such that its utility can be assessed in comparison with that of substances in current clinical use. One simple means is to conduct flow cytometry studies of its effect on the cell cycle, a procedure used by us to determine the effect of bistramide A on a non-small-cell bronchial carcinoma line.

Bistramide A (also known as bistratene, Fig. 1), a dilactam polyether from the New Caledonian urochordate *Lissoclinum bistratum* Sluiter [2, 5], is cytotoxic to normal and tumor cells and produces a rapid toxic effect on the central nervous system that can be attributed to inhibition of the Na^+ channel both at rest and in the inactivated state [3, 6]. The in vivo activity of this substance against slowly developing tumors is currently being studied, particularly in a continuous human non-small-cell lung cancer cell line (NSCLCN6-L16) [7, 9]. The results of the in vitro studies described herein were obtained using this line.

Materials and methods

Bistramide A. Bistramide A (mol. wt., 704 kDa) was isolated from *L. bistratum* collected at Ua island in New Caledonia as previously described [6]. The purity of the substance was determined by mass spectrometry, infrared spectrometry, and HPLC cochromatography.

Cell line and cell culture. The cloned L16 line of NSCLC-N6 cells from a human non-small-cell bronchopulmonary carcinoma (moderately differentiated, rarely keratinizing; classified as T_2NoMo) was used for all determinations. It was grafted into a nude mouse, then cultured in RPMI 1640 medium (Intermed) with 5% fetal calf serum, to which 100 IU penicillin/ml, 100 µg streptomycin/ml, and 2 mm glutamine were added. Cells were cultured at 4×10^5/ml at 37° C in an air-carbon dioxide (95:5, v/v) atmosphere. Under these in vitro conditions, the cell-doubling time was about 32 h, whereas it takes 24 days in vivo.

Cytotoxicity determination. Experiments were performed in microplates (2.1×10^5 cells/ml). Bistramide A was tested at concentrations of 0.35, 1.42, and 7.1 µM. Cell growth was estimated by a colorimetric assay based on conversion of tetrazolium dye (MTT) to a blue formazan product using live mitochondria [8] at 17, 25, 41, 49, and 67 h. Eight determinations were performed for each concentration. Control growth (without bistramide) was estimated from 16 determinations. The confidence intervals in Fig. 2 represent the standard deviations calculated for each of the points.

Flow cytometry assay. For DNA staining, 2.1×10^5 cells were cultured in 25-ml flasks in the absence as well as the presence of 0.35, 0.71, and 1.42 µM bistramide A. Determinations were performed at 24, 45, 74, and 94 h. As the NSCLCN6-L16 line shows a very strong capacity for adherence, DNA staining was carried out using the technique of Vindelov [11]. The cells were directly treated in the flask with the staining solution, which destroys the cytoplasm before staining. After the removal of culture medium, 1 ml Vindelov's solution [0.01 M glycine/NaOH; 9.6×10^{-5} M propidium iodide (Sigma P 5264); 0.1 M Nonidet P-40 (Sigma N 6507); 700 IU ribonuclease A/l (Sigma R 5250); 0.3 M NaCl; pH 10] diluted 1:2 (v/v) in phosphate-buffered saline was dropped into the flasks, which were then shaken and left in a dark environment at 4°C for 15 min. The cell suspension thus obtained was filtered on nylon mesh (50 µm) and analyzed.

All flow cytometry experiments were performed independently eight times. The DNA content of 25,000 naked nuclei was measured by an ATC 3000 flow cytometer (Bruker, Wissembourg, France) connected to an MCA 3000 multichannel analyzer (Bruker). Propidium iodide was excited (488 nm) using an argon laser (Innova 90.5 UV; Coherent Laser Products Division, Palo Alto, Calif.) at 400 mW. Fluorescence was mea-
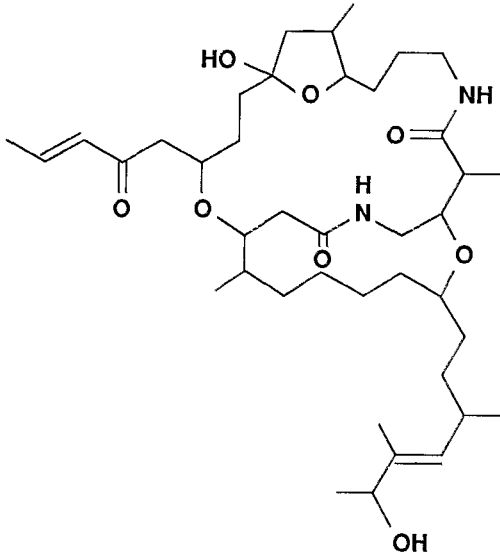
Fig. 1. Structure of bistramide A

sured at wavelengths of >610 nm. To eliminate doublets, nuclei for DNA area histogram analysis were selected by gating on the cytogram "DNA peak vs DNA area".

For flow cytometric analysis, cells that had not been treated with bistramide A the in GO/G1, S, and G2M phases were estimated by the mathematical model of Fried [4]. However, as is often the case, treated cells could not be analyzed by this method. Cell distribution in the cell cycle was thus evaluated by planimetric analysis [1]. Through the use of an additional gate on the DNA fluorescence vs FALS cytogram, the most fluorescent cells were selected to enhance the visualization of residual triplets and to estimate the number of cells whose DNA contained "8C" chromosomes. The cell debris resulting from the action of bistramide A was apparent on the DNA histograms.

Electron microscopy studies. Two cell suspensions of 3 × 10⁵ cells/ml were cultured either with 0.175 µM bistramide or without the drug. After 45 h incubation, cells were collected and resuspended in 1 ml RPMI in Pyrex hemolysis tubes and were then sedimented by mild centrifugation (1,000 rpm) for 10 min. After the removal of culture medium, cell pellets
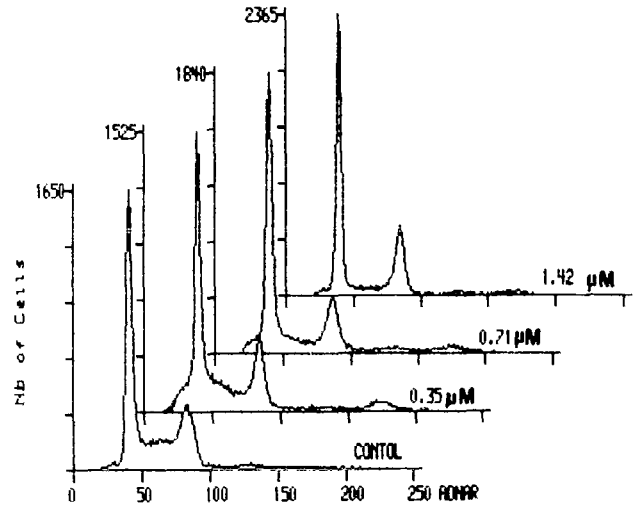
Fig. 3. DNA histogram of NSCLCN6-L16 cells cultured in the presence of different concentrations of bistramide (0.035, 0.71, and 1.42 µM) for 45 h. The decrease in the percentage of S-phase cells is dose-dependent. The percentage of cells of the peak corresponding to "4C" chromosomes varies little, and the number of cells in peak "2C" is also increased in a dose-dependent way as compared with controls. However, in the presence of 0.35 µM bistramide, a peak corresponding to "8C" chromosomes is clearly visible

were fixed at 0 C for 90 min in a 0.3 M, pH 7.2 (370 mosmol), sodium cacodylate-buffered 3% solution of OsO₄ or in a 0.1 M, pH 7.2 (380 mosmol), sodium cacodylate-buffered 2.5% solution of glutaraldehyde. Cells were then washed for 24 h in a solution of 0.1 M sodium cacodylate and 0.4% NaCl. Aggregates fixed in glutaraldehyde were postfixed in OsO₄ under the same conditions described above and were then rewashed.

All specimens were dehydrated in increasing degrees of alcohol, cleared with propylene oxide, and then embedded in Epon 812. Semi-thin (1 µm) and thin (50–70 nm) sections were cut using a Reichert ultramicrotome. Semi-thin sections were stained with toluidine blue and then examined under a Leitz Ortoplan microscope; thin sections were stained with uranyl acetate and lead citrate and were then examined and photographed in a JOEL 100 C electron microscope.
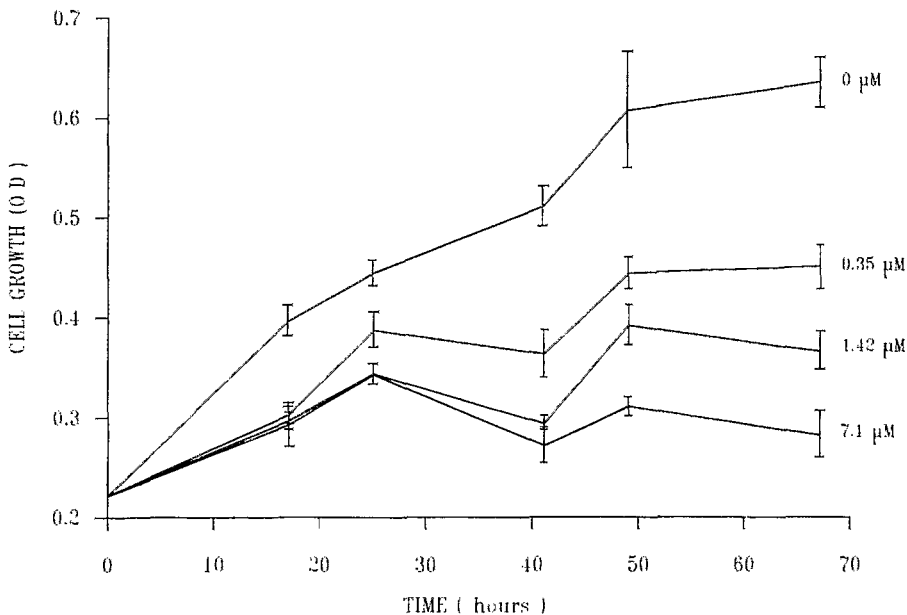
Fig. 2. Effects of bistramide A on NSCLCN6-L16 cell growth as a function of concentration and contact time

a.
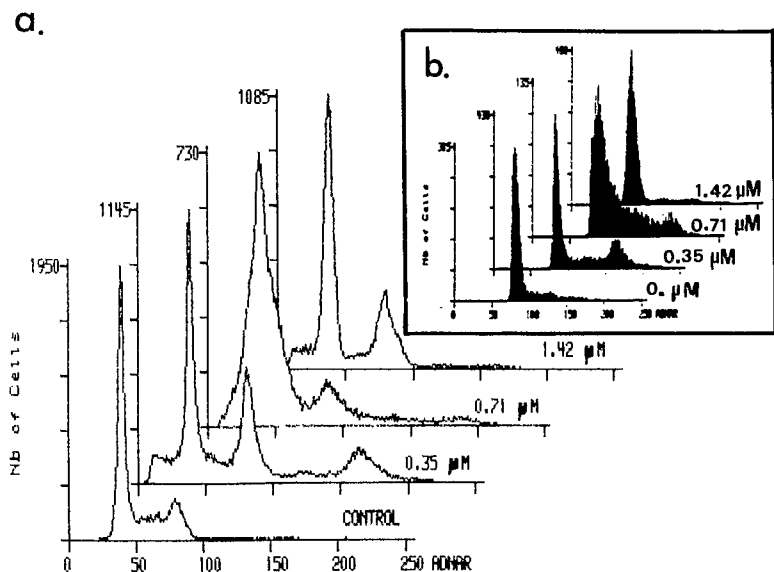
Fig. 4 a, b. DNA histogram of NSCLCN6-L16 cells cultured in the presence of different concentrations of bistramide (0.035, 0.71, and 1.42 µM) for 74 h. **a** After 74 h culture in the presence of bistramide, "damaged" cells are increased and produce considerable debris at 0.71 µM. The effect at 45 h is intensified: "8C" cells are apparent in large number at 0.35 µM bistramide, are nonexistent at 1.42 µM, and occur infrequently at 0.71 µM. **b** By means of an additional gate on the DNA vs FALS cytogram, the most fluorescent cells corresponding to the "4C" and "8C" chromosome peaks are selected to enhance visualization of the "8C" peak as a function of the bistramide concentration used
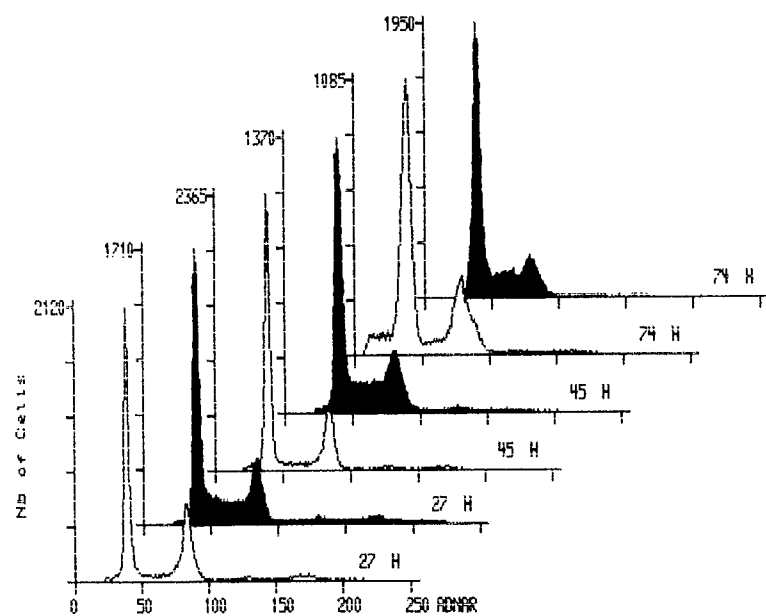
Fig. 5. Effect of 1.42 µM bistramide as a function of culture time (24, 45, or 74 h). ☐, Bistramide; ■, control. Beginning at 24 h, an increase can be noted in the "2C" and "4C" peaks to the detriment of the S phase as compared with the control. With the passage of time, the peak "2C" cells increase, a stable residual S phase subsists, and the percentage of peak "4C" cells decrease. The amount of debris is increased at 74 h, indicating cell mortality
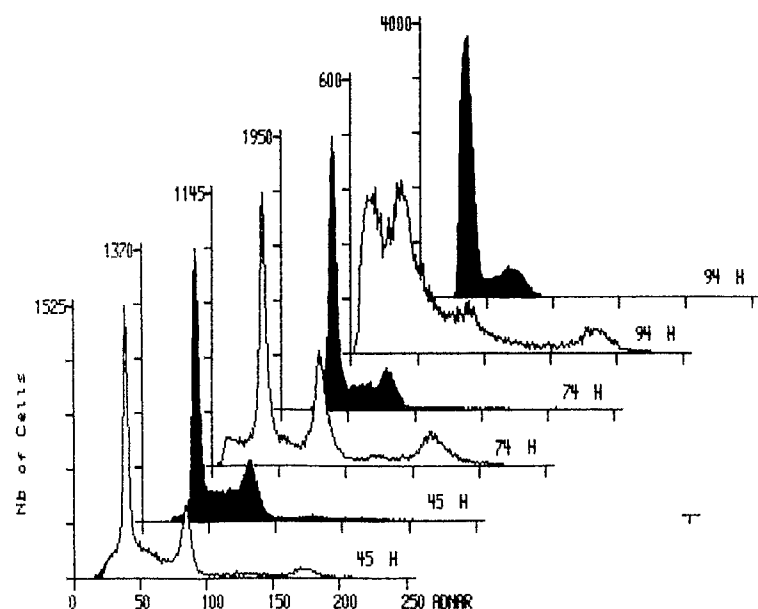
Fig. 6. Effect of 0.35 µM bistramide as a function of culture time (45, 74, or 94 h). ☐, Bistramide; ■, control. At 45 h, 0.35 µM bistramide causes a significant decrease in the number of S-phase cells, the appearance of an "8C" peak, and the persistence of the "4C" peak. At 72 h, an intensification of the phenomenon is visualized, particularly an increase in the "8C" and "4C" peaks. At 94 h, the presence of debris related to high cell mortality partially masks the three peaks ("2C", "4C", and "8C"). The increased CV of the corresponding control "2C" peak is due to a decrease in growth factors in the cell-culture medium
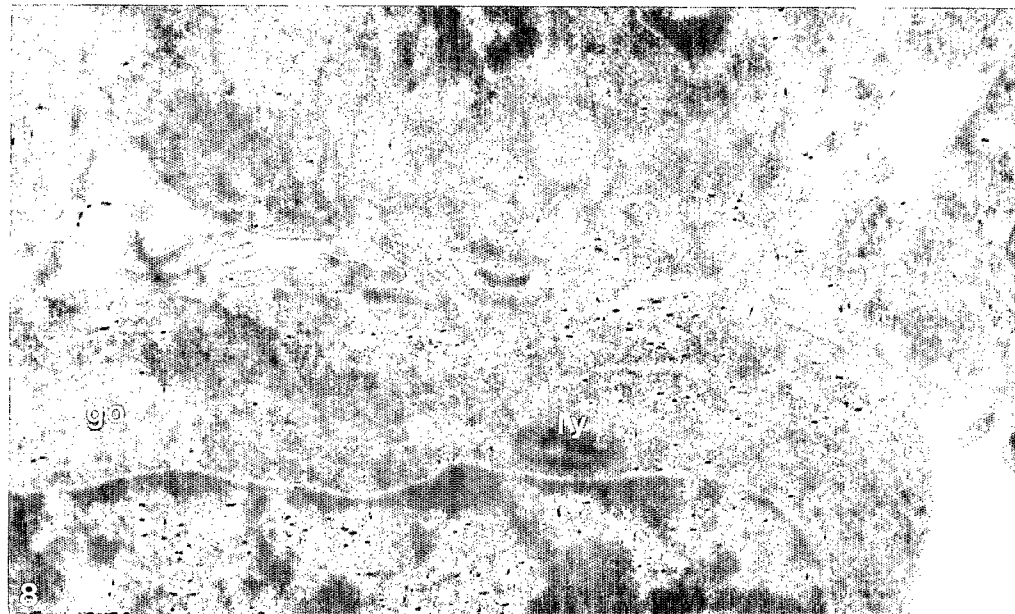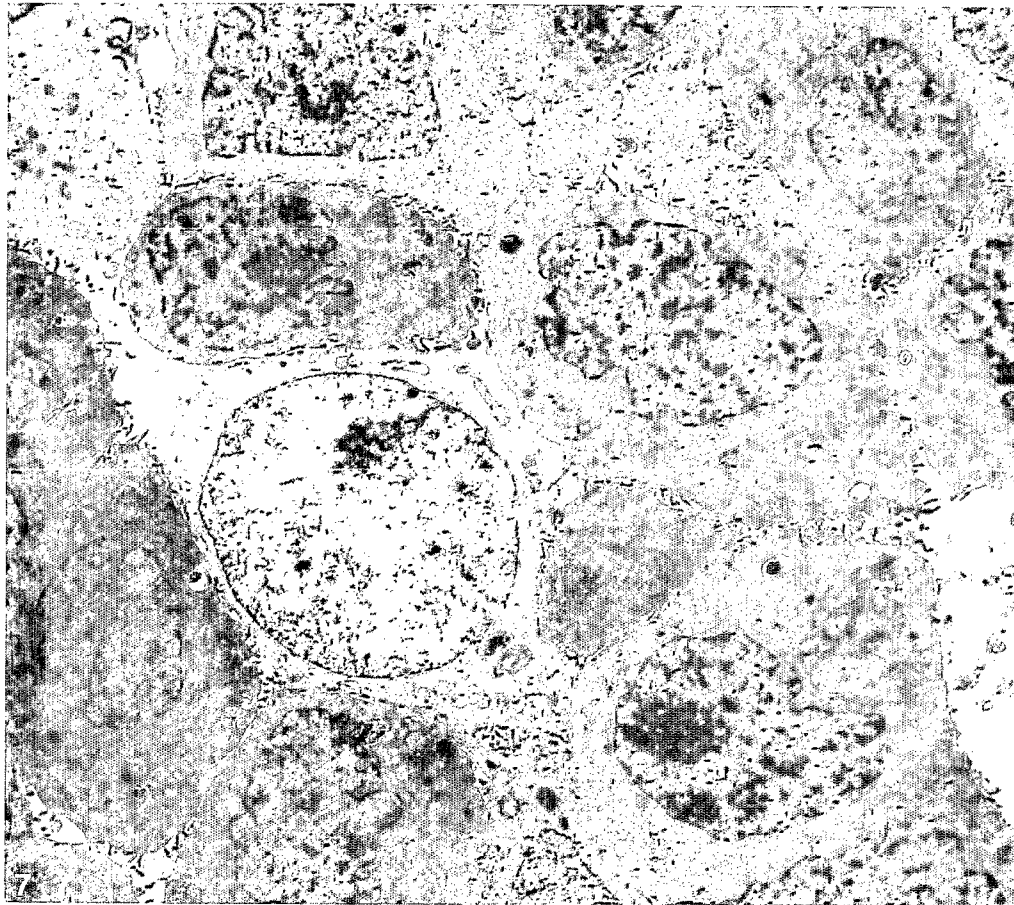
Fig. 7. General view of an untreated tumor-cell culture. The cells produce digitations that mesh with those of adjacent cells and ensure the cohesion of the culture. The cytoplasm is generally dark and the nucleus is slightly notched, with the exception of some larger elements that display a clear cytoplasm and nucleus ×4.200

Fig. 8. Detail of the intercellular meshes between untreated tumor cells. go, Golgi complex; ly, lysosome. ×20.000

Results

Cytotoxicity

Figure 2 shows the growth of NSCLCN6-L16 cells in the absence as well as in the presence of 0.35, 1.42, and 7.1 μM bistramide A as determined at different time points. The concentration of drug required to inhibit cell growth by 50% (IC$_{50}$) was 0.49 μM at 67 h.

Effects on the cell cycle

Figures 3 and 4 show the effects of bistramide A on the cell cycle according to concentration. A blockade of cells in the G1 phase was demonstrated by a dose-dependent decrease in S-phase cells. However, the persistence of a "4C" peak was simultaneously noted G1-phase cells, even following treatment with 1.42 μM bistramide, at 45 (Fig. 3) and 74 h (Fig. 4a). At lower concentrations (0.35 and 0.71 μM), partial blockade occurred in the G1 phase along with the appearance of polyploidy.

Figures 5 and 6 illustrate the time-dependent effects of bistramide A on the cell cycle. A blockade of G1-phase cells was noted at 24 h following treatment with 1.42 μM drug (Fig. 5). At between 4 and 24 h, the percentage of S-phase cells decreased in a time-dependent manner (data not shown). At the time at which bistramide was added, S-phase cells of the asynchronous culture continued their progression in the cell cycle, and a nearly stable state was maintained from 24 h on at a drug concentration of 1.42 μM. The appearance of debris and the increased coefficient of variation (CV) of the "2C" peak at 74 h could be considered to be indices of cell mortality. However, in the presence of 0.35 μM bistramide A (Fig. 6), partial G1-phase blockade and the appearance of polyploidy were significant from 45 h onward. These two effects were even more marked at 72 h, whereas extremely high cell mortality was observed at 94 h.

Ultrastructural analysis

The series of ultrastructural images showed that in the absence of bistramide treatment tumor cells form interdependent groups (Fig. 7) and that isolated cells occur infrequently. The phenomena of intracellular recognition are such that the cells produce peripheral digitations that mesh with those of adjacent cells (Fig. 8). The cells are thus squeezed against each other, becoming deformed by their mutual pressure. Images indicating lysis or cell degeneration were extremely rare. Signs of mitosis could be observed, albeit infrequently, and attested essentially to the asynchronism of the culture, which was corroborated by the variable features of elements in cells that were in an interphasic state (Fig. 9). In fact, most of the cells displayed a dark, reduced cytoplasm, with only a few showing a larger, clear cytoplasm that was richer in differentiated cell constituents. The most remarkable of these constituents involved the mitochondria (Fig. 10), which were often seen in association with lipid droplets (1–2 μm in diame-

ter) and displayed a reduced size (0.5–1 μm) in nearly all tumor cells (Fig. 11). Some cells also contained very clear vacuoles (never more than 3–4 μm in diameter) lined with microfilaments.

Cultivation of tumor cells in the presence of high drug concentrations (1.4 μM) led to cell death and, hence, to the absolute impossibility of analyzing cells ultrastructurally. When concentrations of 0.175–0.35 μM were used, important changes took place in the behavior of the cell culture. Cell degeneration and necrosis occurred more frequently, and the heterogeneity of the features observed in living cells was remarkable. There were many isolated cells in which elements undergoing mitosis were frequently seen. Cell groups were also observed, with the digitations being essentially responsible for the adhesion process. However, in the presence of bistramide, there was differentiation of specialized junctions such as desmosomes (Figs. 12, 13). When these ultrastructures were present, the plasma membranes of two adjacent cells put vast areas of parallel linear membrane into common use by providing a narrow intercellular space. Specific receptor-exchange phenomena probably occurred between adjacent cells under these conditions, since clathrine-coated cytosis vesicles could be found (Fig. 13).

The lipid droplets and clear vacuoles scattered through the hyaloplasm did not disappear but were less frequently observed. The chondriome of many cells was found against the nuclear membrane around the nucleus. Everything in this respect occurred as if the available energy were focused on the nuclear material, presumably in preparation for cell division (Fig. 15). Other cells contained mitochondria showing unusual features of size (7–8 μm and sometimes larger) and shape and an anarchic arrangement of the crests (Fig. 14). Internal cavities also appeared in treated tumor cells. These cavities were very large (sometimes >15 μm) and were lined with microvilli. However, the slightly opaque content of the electrons was different from than that observed in intercellular spaces. Close study of these internal cavities would probably be of considerable interest but did not lie within the scope of the present work. Nonetheless, it may at least be deduced from our observations that the cavities correspond to a particular production of bistramide-treated tumor cells. Cavities delimited by two or three cells grouped in pseudoglandular formation were also noted (Fig. 12).

At a bistramide concentration of 0.35 μM, cell sections exhibiting two nuclei separated by a hyaloplasmic layer of variable thickness (sometimes very thin) were quite frequently seen (Fig. 12). These were not different sections of the same notched nucleus, since such sections would have had very regular and roughly rounded contours. It is true that nuclei with a very irregular and notched contour could also be observed, but they composed only a minority of the nuclear population. Cell sections with three and even four nuclear sections were assiduously sought and found (Fig. 17). Given the scale at which our observations were carried out, it is true that nuclei were not always included in a section and that the presence of three nuclear sections in the same cell most often implied the presence of at least four nuclei. However, the possibility that the cells had an uneven number of nuclei (e.g., three) cannot be excluded.
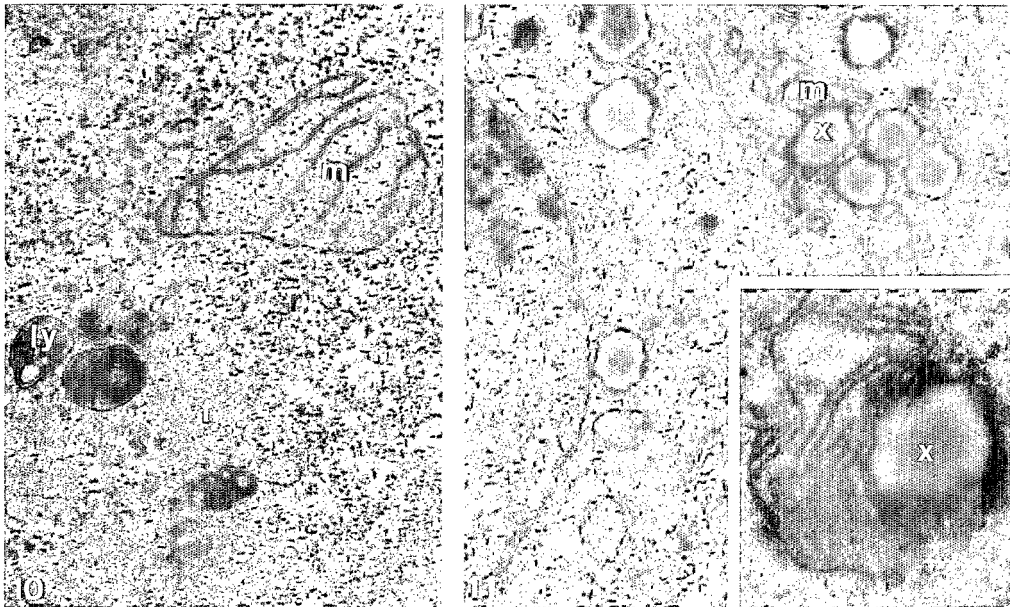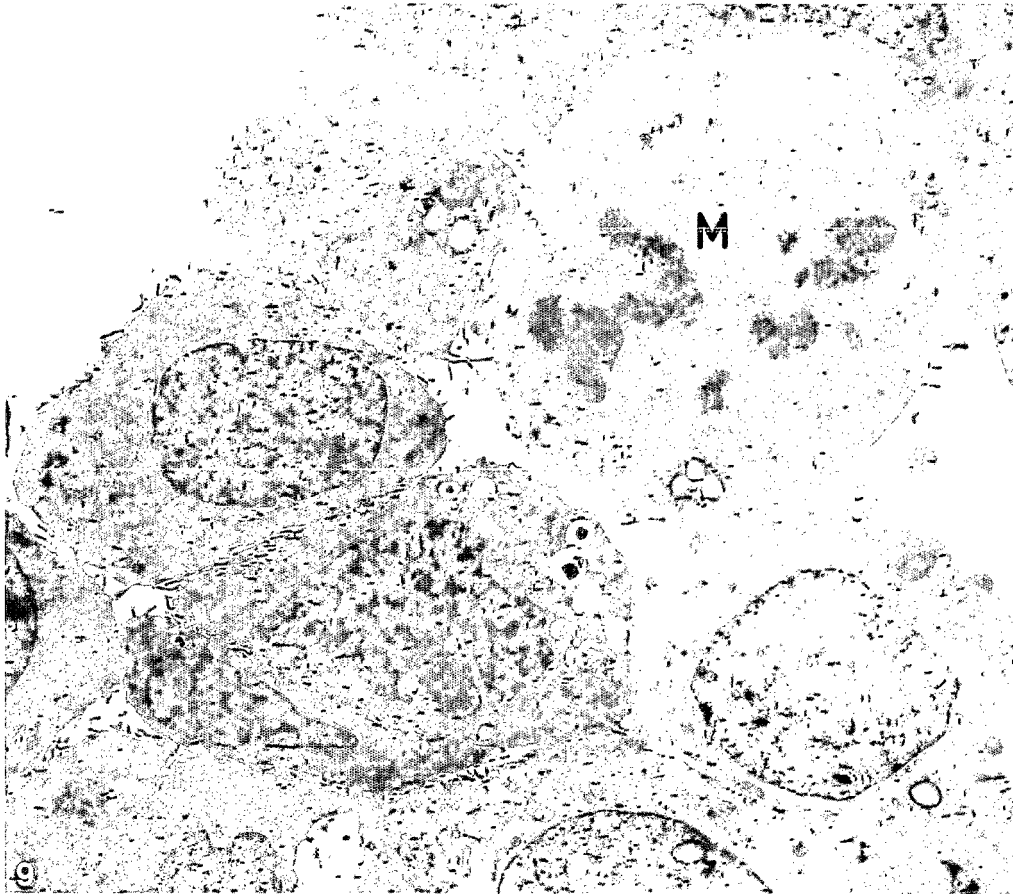
Fig. 9. General view of an untreated tumor-cell culture: signs of mitosis (*M*) can be infrequently observed. × 4,200

Fig. 10. Portion of an untreated tumor cell. *m.* Mitochondria: *f.* filament: *r.* ribosomes: *ly.* lysosomes. × 21,000

Fig. 11. Tumor cells frequently contain lipid droplets (*x*) associated with mitochondria (*m*). × 6,500. *Inset:* Detail of a mitochondrion squeezed against a lipid droplet. × 21,000
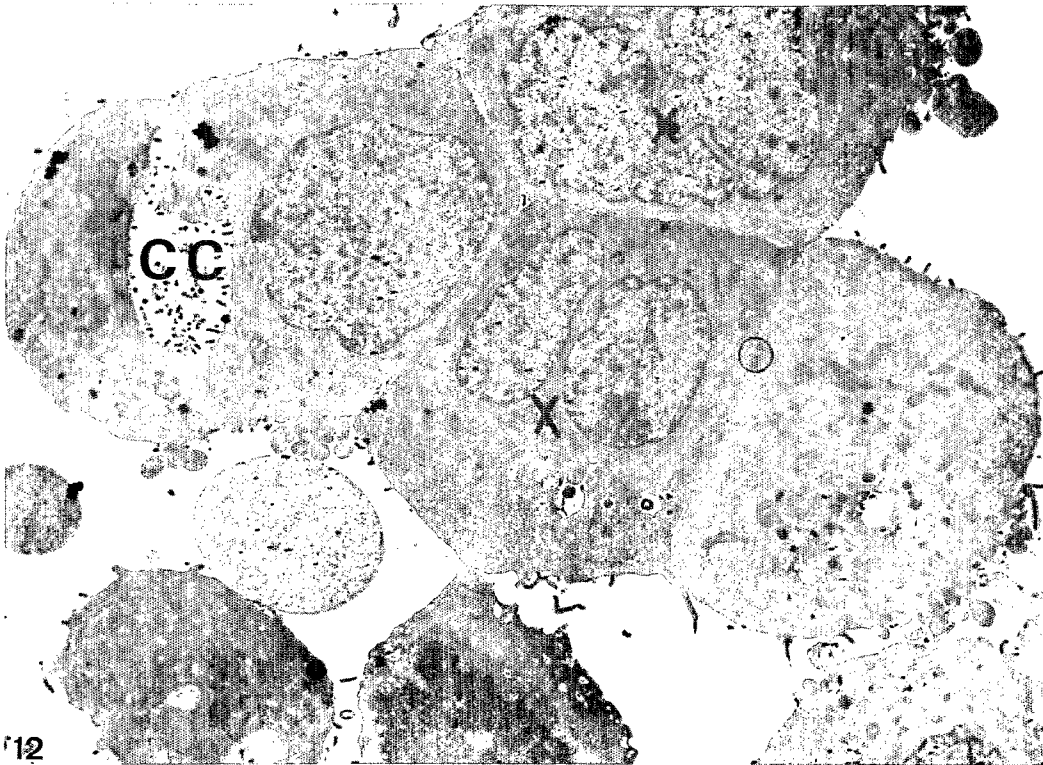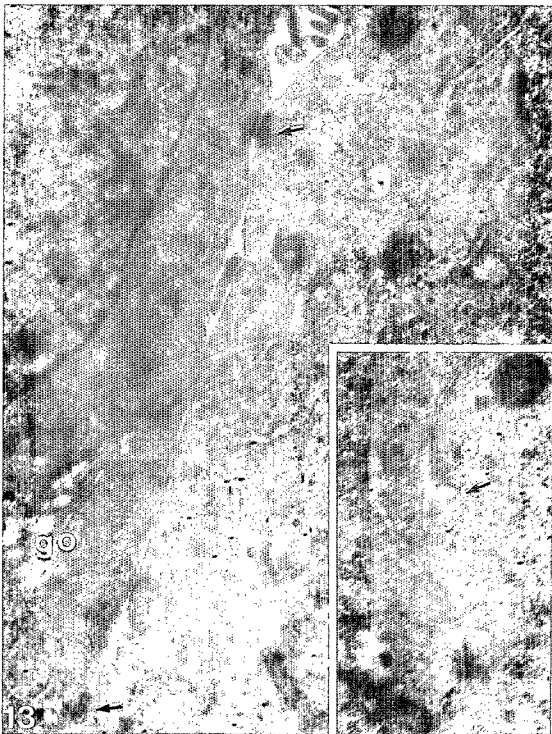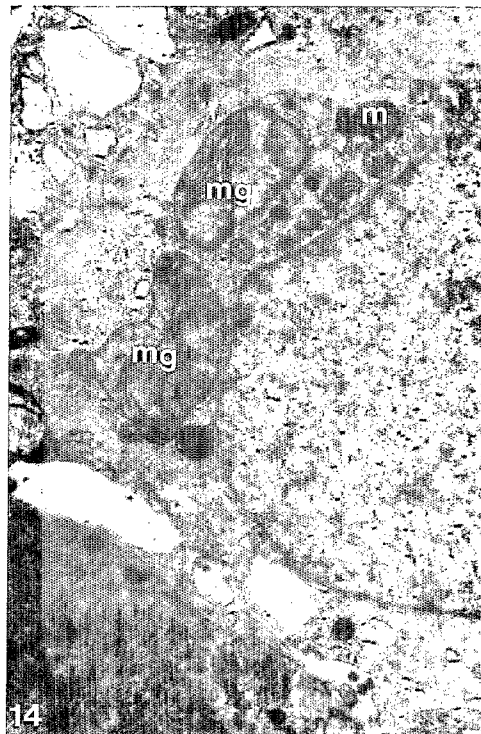
Fig. 12. General view of a tumor-cell culture treated with bistramide (0.35 μM medium). Two binuclear cells (*x*) and two cells in pseudoglandular formation surround a central cavity (*CC*). Three desmosomes (*circle*) can be seen in this group of four very interdependent cells. × 4,200

Fig. 13. Detail of the intercellular junctions, showing two characteristic desmosomes (*arrows*). *go*, Golgi complex. *Inset:* Detail of a coated vesicle (*arrow*) and another desmosome. × 12,000

Fig. 14. Portion of a tumor cell treated with 0.35 μM bistramide. Two giant mitochondria (*mg*) are visible next to mitochondria of normal size (*m*). × 7,000

16 **17**
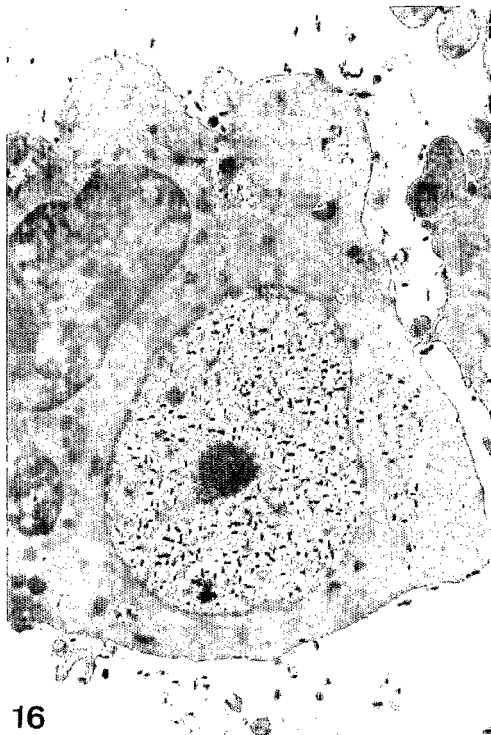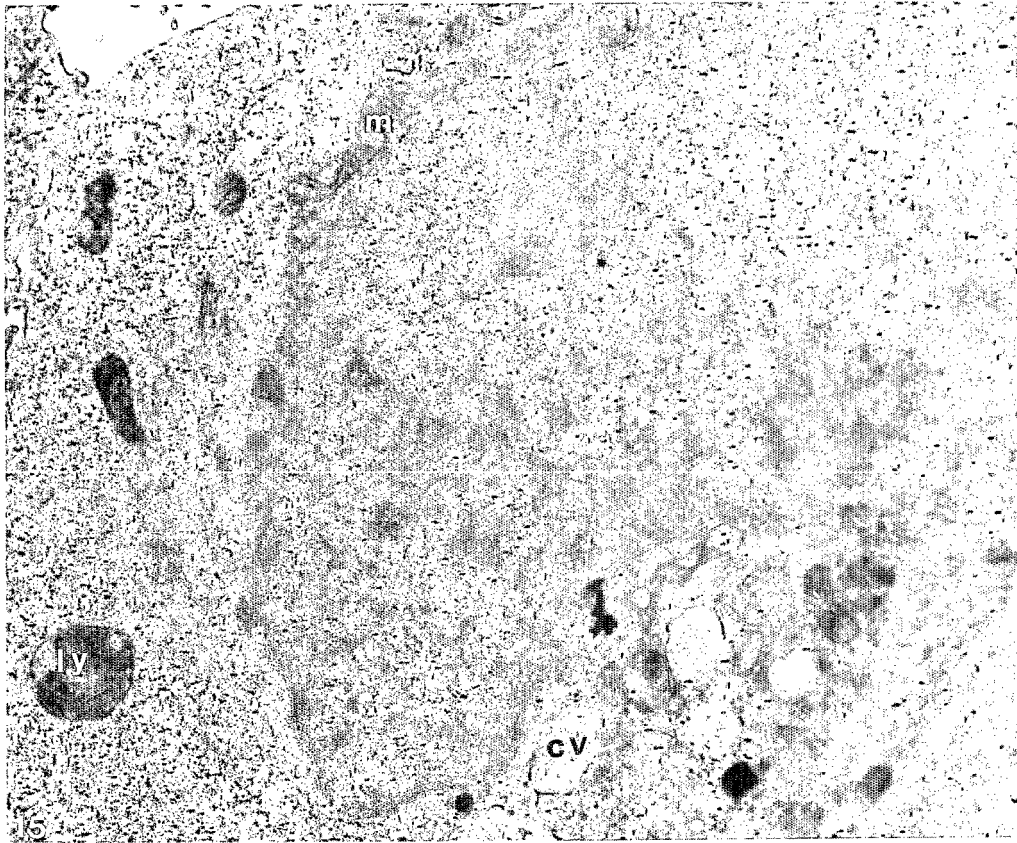
Fig. 15. Portion of a tumor cell treated with 0.35 μM bistramide. Mitochondria (m) are squeezed against the nuclear membrane. cv. Clear vacuole; ly. lysosome. × 11.000
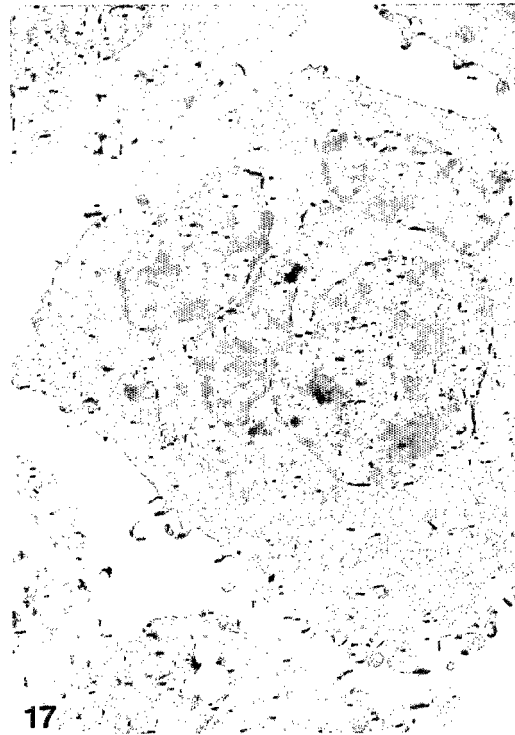
Fig. 16. Tumor cell treated with 0.35 μM bistramide. showing two nuclei with very different features. × 6.700

Fig. 17. Tumor cell treated with 0.35 μM bistramide. exhibiting four nuclear sections. × 6.000

If the karyokinetic stages occurring after the first one are asynchronous, the cell involved must necessarily contain an uneven number of nuclei at a given moment. In fact, we observed a cell containing two nuclei that were at very different stages of maturation (Fig. 16). In general, it may be that nuclear but not cellular divisions are possible in a tumor-cell culture in the presence of low concentrations of bistramide: karyokinesis is apparently not followed by cytokinesis.

Discussion

As previously demonstrated [3, 6], bistramide A has dose-dependent cytotoxic properties, particularly for the NSCLC line. The content of DNA in flow cytometry studies was proportional to the intensity of cell fluorescence and, thus, to the quantity of intercalary fluorochrome fixed by the double strands of DNA. Consequently, GO- and G1-phase cells were indistinguishable from each other, as were G2/M-phase cells from "2C" doublets or binuclear cells. In fact, nuclear staining using the technique of Vindelov [11] does not lead to total destruction of the cytoplasm, the result being that the nuclei of binuclear or polyploid cells are not dissociated. This was confirmed by fluorescence microscopic observation of the suspension analyzed in flow cytometry.

Despite the gate provided on the cytogram "DNA area vs DNA peak", doublets and triplets were analyzed as if they were single cells with "4C" or "6C" chromosomes. The presence of residual triplets on the treated cells and the control histogram was easily detectable and enabled the overestimated number of "4C" or "8C" cells to be corrected. In the interpretation of the results, this factor of error was taken into account. However, it may have only reflected mitotic asynchronism subsequent to the first division of treated cells. The ultrastructural data are entirely compatible with this interpretation.

During study of the mode of action of a drug, when culture times are long, cell mortality is normal and debris appears. If the debris were eliminated by a gate on the FALS vs DNA peak or the FALS vs WALS cytograms, S-phase overestimation would be possible. Therefore, it seemed preferable to let the debris appear, to the detriment of the appearance of the DNA histogram. Elimination of this debris would have been possible by mathematical treatment of the histograms, but too many data would have been removed logarithmically and the resulting histogram would not have been reliable.

The results of this study clearly show the antiproliferative effect of bistramide on asynchronous cultures of the cloned line (NSCLCN6-L16) through its action on the cell cycle. Bistramide acts by a dual mechanism involving the blockade of G1-phase cells and the appearance of polyploidy that is suggestive of inaptitude for cytodieresis.

The blockade of G1-phase cells is in agreement with the results of previous studies in which this molecule was presented as an agent of cell differentiation with respect to non-small-cell bronchial carcinomas [10] and, in certain aspects, to the HL 60 monocytic line of leukemic origin [12]. This hypothesis is also supported by the morphologi-cal modifications assimilable to cell maturation in the NSCLCN6-L16 line after treatment with 0.35 μM bistramide for 45 h: the appearance of junction systems such as desmosomes after the plasma membranes of adjacent cells have been brought closer together is highly suggestive of cell maturation. Likewise, the presence of coated vesicles attests to a process of differentiation as well as to intercellular communication. However, the general phenomena described herein are not definitive markers of differentiation. This potential property of NSCLC requires more thorough investigation. Furthermore, we also considered in detail the potential differentiating properties of this substance on NSCLC.

The induction of polyploidy by bistramide, which seems to be inversely proportional to the concentration used, is in fact simply the result of dose-dependent blockade of G1-phase cells and of the incapacity of cells to achieve cytodieresis. At low concentrations, cells that are not blocked in the G1 phase ("2C") attain the G2M phase. Their incapacity to divide leads to the entry of binuclear cells ("4C") into the cell cycle, some of which are partially blocked in the G1 phase, with a resulting increase in the intensity of the "4C" peak. This process also occurs in nonblocked cells, resulting in the appearance of a quadrinuclear cell peak ("8C"). This polyploidy was confirmed by electron microscopy studies.

The study of the cell cycle as a function of bistramide concentration and contact time thus shows that inhibition of cytodieresis occurs at doses lower than those inducing maximal blockade of G1-phase cells by a putative differentiation process.

References

1. Barlogie B, Drewinko B, Johnston DA, Buchner T, Hauss WH, Freireich EJ (1976) Pulse cytophotometric analysis of synchronised cells in vitro. Cancer Res 36: 1176–1181
2. Degan BM, Hawkins CH, Lavin MF (1989) Novel cytotoxic compounds from the ascidian *Lissoclinum bistratum*. J Med Chem 32: 1354–1359
3. Ecault E, Gouiffes-Barbin D, Sauviat MP, Verbist JF (1991) Blockade of sodium channels by bistramide A in voltage-clamped frog skeletal muscle fibres. Biochem Biophys Acta (in press)
4. Fried J, Mandel M (1979) Multi-user system for analysis of data from flow cytometry. Comput Programs Biomed 10: 218–230
5. Gouiffes D, Moreau S, Helbecque N, Bernier JL, Henichart JP, Barbin Y, Laurent D, Verbist JF (1988) Proton nuclear magnetic study of bistramide A, a new cytotoxic drug isolated from *Lissoclinum bistratum* Sluiter. Tetrahedron 44: 451–459
6. Gouiffes D, Jugé M, Grimaud N, Wellin L, Gauviat MP, Barbin V, Laurent D, Roussakis C, Henichart JP, Verbist JF (1988) Bistramide A, a new toxin from the Urochordata *Lissoclinum bistratum* Sluiter: isolation and preliminary characterization. Toxicon 26: 1129–1136
7. Gratas C, Robillard N, Roussakis C, Audouin AF, Verbist JF (1990) Study of the heterogeneity of a human non-small-cell bronchopulmonary epidermoid primary carcinoma: determination of the DNA content of NSCLCN6L2 cells and of cloned sub-populations. Biol Cell 68: 133–138

8. Mosmann T (1983) Rapid colorimetric assay for cellular growth and survival: application to proliferation and cytotoxicity assays. J Immunol Methods 65: 55–63

9. Roussakis C, Dabouis G, Gratas C, Audouin AF, Viaud P, Lemevel B (1986) Establishment in culture of a bronchial epidermoid carcinoma cell line of human origin (abstract 248). Proceedings, 5th NCI-EORTC symposium on new drugs in cancer therapy. Amsterdam; 12th Congress of the European Society for Medical Oncology. Nice

10. Roussakis C, Gratas C, Chinou I, Audouin AF, Robillard N, Gouiffes D, Bourget G, Verbist JF (1989) Activité différenciatrice de deux substances naturelles: le Cu₁ et le bistramide vis-à-vis des NSCLC in vitro. Bull Cancer 76: 478–479

11. Vindelov LL (1977) Flow microfluorometric analysis of nuclear DNA in cells from solid tumors and cell suspensions. A new method for rapid isolation and staining of nuclei. Virchows Arch [Cell Pathol] 24: 227–242

12. Watters D, Marshall K, Hamilton S, Michael J, McArthur M, Seymour G, Hawkins C, Gardiner R, Lavin M (1990) The bistratenes: new cytotoxic marine macrolides which induce some properties indicative of differentiation in HL-60 cells. Biochem Pharmacol 39: 1609–1614